

## Effect of pulse time on surface characteristics and corrosion resistance during pulse electrochemical polishing

Young-Bin KIM<sup>1</sup>, Jeong-Woo PARK<sup>2</sup>

1. Department of Advanced Parts and Materials Engineering, Chosun University, Gwangju 501-759, Korea;

2. Department of Mechanical Design Engineering, Chosun University, Gwangju 501-759, Korea

Received 21 May 2012; accepted 13 August 2012

**Abstract:** Pulse electrochemical polishing (PECP) was used to improve the mechanical properties, such as surface roughness and corrosion resistance, of conductive metallic materials. PECP can provide a smooth, bright, reflective, and deburred surface that exhibits superior corrosion resistance. In this work, stainless steel was used as the anode, and copper was used as the cathode due to their low electrical resistances. The surface roughness of the PECP sample was measured by atomic force microscopy (AFM). A scanning electron microscope (SEM) was used to observe surface characteristics, and an Auger electron spectroscopy (AES) was used to analyze the metallurgical composition and thickness of the passive film. The aim of this research was to compare the corrosion resistance rates of the unprocessed and PECP-processed stainless steel.

**Key words:** stainless steel; pulse electrochemical polishing; corrosion resistance

### 1 Introduction

The growing importance of precision, cleanliness, and resistance of materials used in the automobile, aircraft, and vessel industries requires process development in the production of semiconductors and liquid crystal displays (LCD). Thus, in order to improve the smoothness, cleanliness, and corrosion resistance of surface structures, a non-contact processing method of electrochemical polishing (ECP) has become a necessary alternative to existing mechanical polishing methods that require contact between tools and structures [1]. Generally, the mechanical polishing methods produce tiny processing traces, such as burr on the surface of structures, and fundamentally precise and robust surfaces cannot be obtained [2]. However, when a non-contact surface processing method of ECP is used, improvements in tiny processing trace, roughness, resistance, and cleanliness of the structure surfaces are reported. ECP processes the surface using current density similar to mirror-like finishes. However, when low level current density is used, black corrosion will be observed on the surface of the structure. Low level current density allows detailed processing of areas that cannot be processed

through mechanical polishing methods; therefore, it is expected to improve surfaces compared with existing mechanical processing methods. In this work, the effect of pulse time on corrosion resistance rate against synthetic sea water and surface characteristics after pulse electrochemical polishing (PECP) was investigated.

### 2 Principle of pulse electrochemical polishing process

Figure 1 illustrates the experimental sequence used in this work. PECP involves the melting of an anode by an electrochemical reaction initiated through the application of a pulse power supply in the ECP process. The anode and cathode are submerged in an acidic electrolyte that is either flowing or stationary. Insoluble and low-electrical-resistant copper is used as the cathode electrode. When a pulse current is sent to the two electrodes in an electrolyte, the melting process occurs in the anode (Fig. 2). At this time, a small quantity of oxygen gas is generated on the surface of the anode, and hydrogen gas is generated on the surface of the cathode. Through this melting process, PECP can cover the concave area of a structure surface with protective oxidation layers to prevent melting, and current is

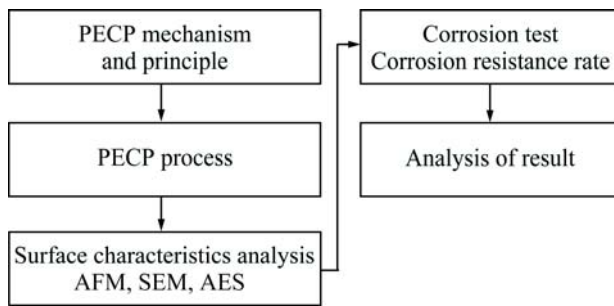


Fig. 1 Diagram of experimental procedure

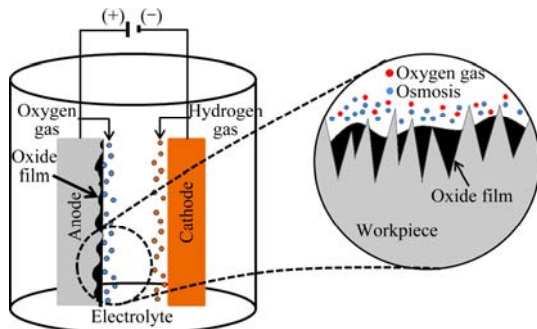


Fig. 2 Principle of ECP

concentrated in the bulging area, enabling selective melting [3,4].

### 3 Pulse electrochemical polishing

The resistance rates for synthetic sea water before and after ECP processing were examined using a pulse power supply. Figure 3 shows a schematic diagram of the PECP experimental setup used in this work. The electrolyte was a mixture of 2.4 mol/L  $\text{H}_2\text{SO}_4$ , 5.9 mol/L  $\text{H}_3\text{PO}_4$ , and distilled water [5]. A 0.3 mm-thick piece of stainless steel 316L measured to be 10 mm  $\times$  100 mm was used as the anode. The copper cathode was 1 mm thick and measured to be 10 mm  $\times$  100 mm. Before local surface processing of a test piece, nitrocellulose was spread on its surface, except for a 5 mm  $\times$  5 mm area, to prevent the electrolyte penetration. A pulse power supply with an output of 50 V and 12 A was used. In order to monitor the voltage and ripple marks of a pulse when conducting PECP processing, a DSO1024 oscilloscope (Agilent Technologies, 200 MHz, 2 GSa/s) was connected to the voltage probe (Agilent Technologies, 300 V) and current probe (Tektronix, 1 mV/mA, 50  $\Omega$ ). A scanning electron microscope (SEM, FEI Company) was used to comparatively analyze the surface shapes, and the component analysis (Thermo Electron Corporation MICROLAB 350) was carried out before and after PECP. The fine surface of the processed specimen was measured locally using an atomic force microscope (AFM, XE-100, PISA).

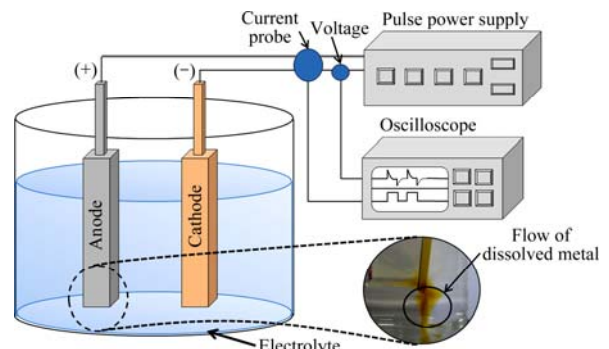


Fig. 3 Schematic diagram of PECP experimental setup

### 4 Surface analysis

Figure 4(a) shows AFM results of the unprocessed specimen. Its surface is extremely rough, and it is found to have a form matching the SEM image in Fig. 4(b). In

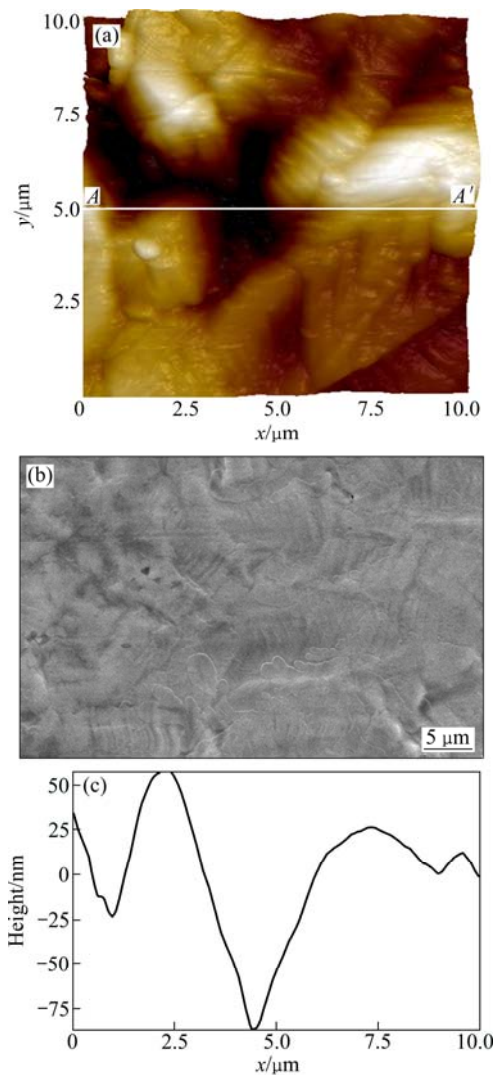
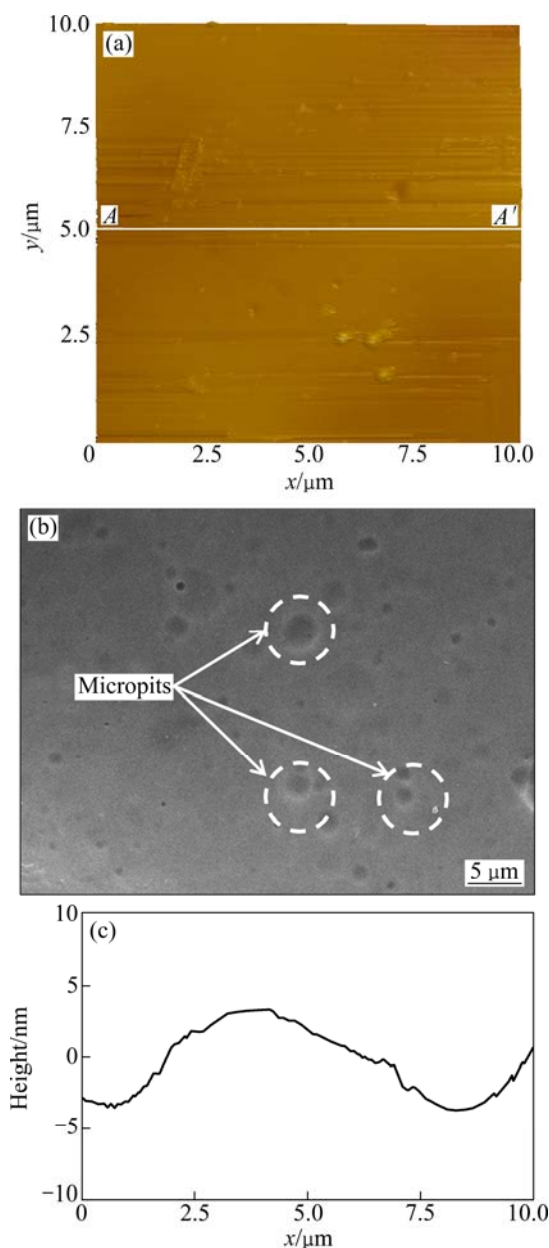


Fig. 4 Sample surface before PECP: (a) AFM topographical image; (b) SEM image; (c) Cross-sectional profile along AA' ( $R_a=27.6$  nm) in Fig. 4(a)

Fig. 4(c), the profile section measured using AFM shows that the surface is severely curved.

Figure 5 shows the results of surface processing with pulse duration of 0.1 ms. Fig. 5(a) shows an AFM image that shows the formation of many micropits. These micropits are likely to corrode and roughen the surface and affect its cleanliness in the future. Fig. 5(b) shows an SEM image that also shows many micropits. In Fig. 5(c), the profile section measured using AFM shows that the specimen surface becomes smoother than the unprocessed specimen surface, but it is highly curved.

Figure 6 shows the results of surface processing with pulse time of 0.8 ms. The AFM image in Fig. 6(a)

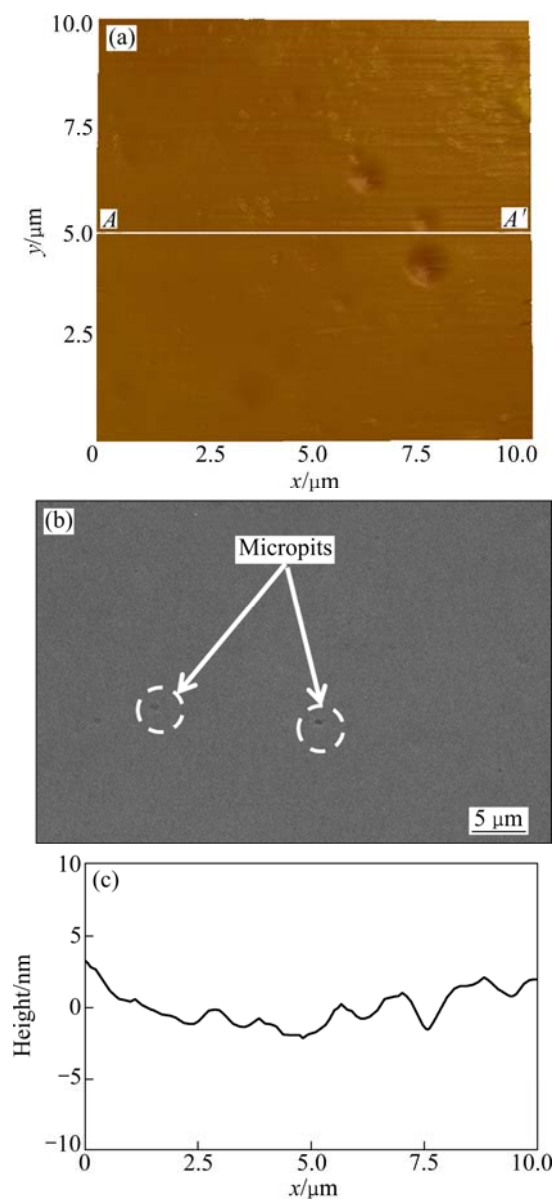


**Fig. 5** Sample surface after PECP (425 Hz, 7 V, pulse time 0.1 ms, process time 180 s, electrode gap 10 mm): (a) AFM topographical image; (b) SEM image; (c) Cross-sectional profile along AA' ( $R_a=2.1$  nm) in Fig. 5(a)

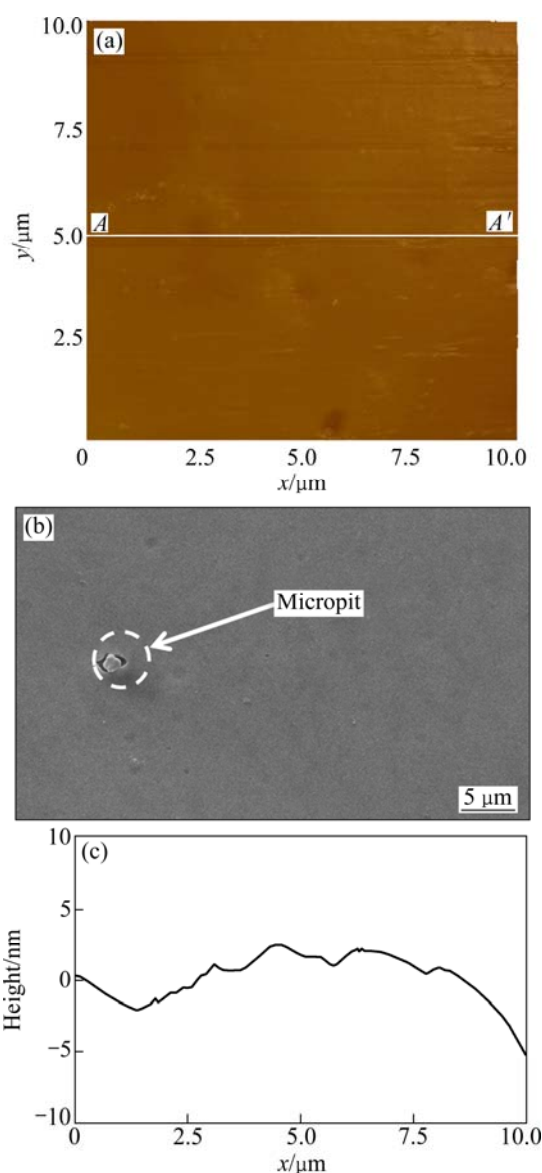
shows few micropits on the surface, confirmed by the SEM image in Fig. 6(b). The AFM profile section in Fig. 6(c) shows that the specimen is slightly curved.

Figure 7 shows the results of a specimen processed with a pulse time of 1.6 ms. It is slightly curved overall, as shown in the AFM image in Fig. 7(a), and it contains many micropits. The SEM image in Fig. 7(b) also shows many micropits created on the surface from processing. A profile of the surface cross-sections in Fig. 7(c) shows the formation of slight curves across the curved specimen.

Figure 8 shows the result of a specimen processed with a pulse time of 2.2 ms. The AFM image in Fig. 8(a)



**Fig. 6** Sample surface after PECP (425 Hz, 7 V, pulse time 0.8 ms, process time 180 s, electrode gap 10 mm): (a) AFM topographical image; (b) SEM image; (c) Cross-sectional profile along AA' ( $R_a=0.7$  nm) in Fig. 6(a)



**Fig. 7** Sample surface after PECP (425 Hz, 7 V, pulse time 1.6 ms, process time 180 s, electrode gap 10 mm): (a) AFM topographical image; (b) SEM image; (c) Cross-sectional profile along AA' ( $R_a=1.3$  nm) in Fig. 7(a)

shows a very rough surface. The SEM image in Fig. 8(b) shows a large number of micropits. These micropits can affect the corrosion resistance by inducing pitting corrosion in the future. A profile of the surface cross-section in Fig. 8(c) shows that an irregular surface forms.

Figure 9 shows the components of the test specimens analyzed before and after processing, determined by Auger electron spectroscopy (AES). The results indicate great increase in oxygen, which induces most of chromium and nickels, is changed to stable passivated oxide layer on the surface. Moreover, it can be seen that the amount of chromium and nickel slightly increases after PECP.

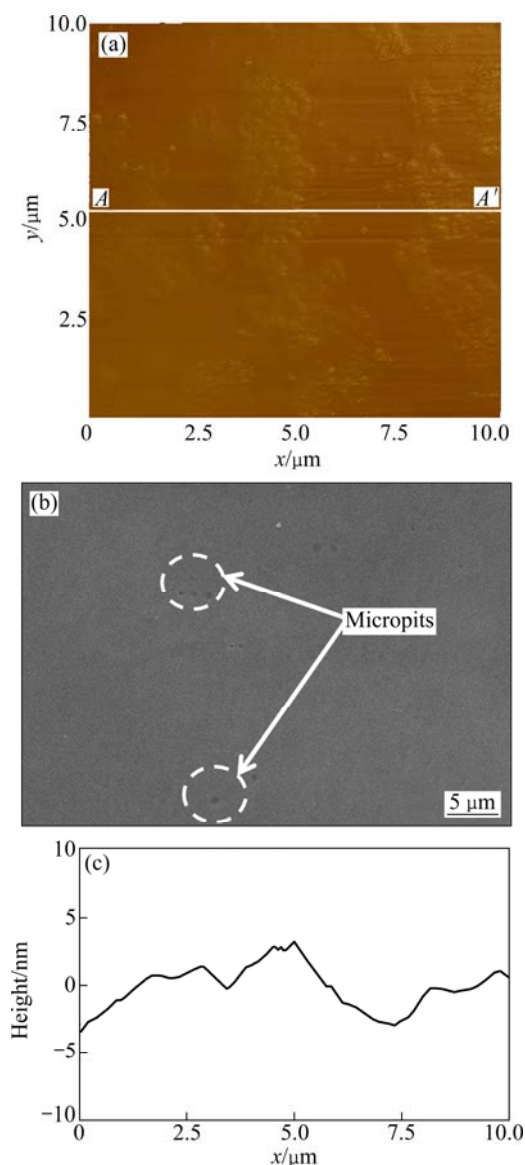


**Fig. 8** Sample surface after PECP (425 Hz, 7 V, pulse time 2.2 ms, process time 180 s, electrode gap 10 mm): (a) AFM topographical image; (b) SEM image; (c) Cross-sectional profile along AA' ( $R_a=1.1$  nm) in Fig. 8(a)

## 5 Corrosion resistance analysis

The corrosion resistance rates of the PECP processed stainless steel 316L specimens were measured and the surfaces of the processed and unprocessed specimens were compared. Sealing tape and silicon were used to cover the area around 5 mm × 5 mm on the specimens. Then, the test pieces were soaked in cells to test the corrosion resistance rate. A 0.05989 mol/L NaCl solution was used to simulate seawater. The oxygen removal period in the cell for the measurement of the resistance rate was 1 h. Electrode washing was then carried out at −1 V for 300 s. The initial voltage for the resistance test was −3 V and ended at 1.5 V. A saturated calomel electrode (SCE) was used as the standard



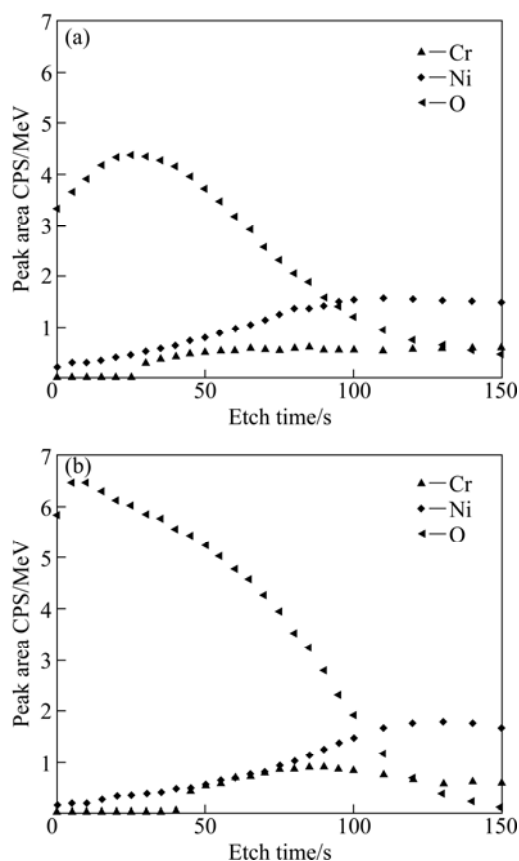


Fig. 9 AES depth profiles: (a) Before PECP; (b) After PECP

electrode, and a 0.05989 mol/L NaCl solution was used to simulate seawater under steady scan rate of 1 mV/s. By using a negative pole polarization curve from the potential dynamic polarization curve, Tafel extrapolation was used to measure the resistance rate [6–8].

Figure 10 shows the Tafel curve of the test specimens tested for corrosion resistance against synthetic seawater with respect to pulse time. The  $x$ -axis on the Tafel curve shows the current density, and the  $y$ -axis shows the potential [9], the corrosion resistance improved as the current density drops. Further analysis

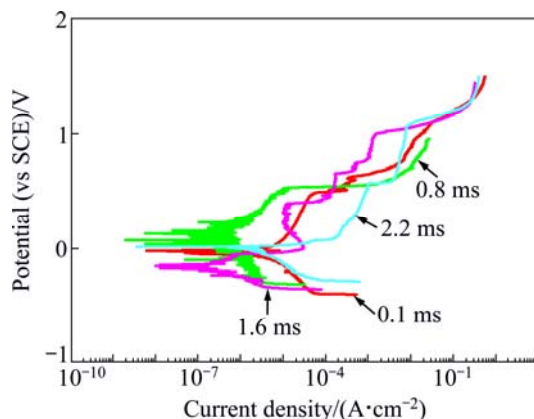


Fig. 10 Corrosion resistance results for unprocessed and PECP-processed specimens

of the Tafel curve indicates that micropit corrosion occurs. It is also confirmed that the test specimen processes with a pulse duration of 0.8 ms can improve the corrosion resistance compared with the test specimens processed with other pulse times.

## 6 Conclusions

1) The surface properties of stainless steel 316L were determined when subjected to PECP processing for various pulse times. The corrosion resistance rate of the specimens processed in synthetic seawater (0.05989 mol/L NaCl) was also examined.

2) The surface of the specimen processed with pulse time of 0.8 ms exhibits the most improvement.

3) A clean surface cannot be produced with short pulse times. According to AES analysis, oxygen content greatly increases while chrome and nickel contents increase after PECP, which indicates the formation of stable passivated layer on the sample surface.

4) PECP with 0.8 ms enhances the corrosion resistance compared with the test specimens processed with other pulse times.

## References

- [1] PARK J W, LEE D W. Pulse electrochemical polishing for microrecesses based on a coulometric analysis [J]. The International Journal of Advanced Manufacturing Technology, 2009, 40: 742–748.
- [2] HAN S J, SEO Y J. Voltage-induced material removal mechanism of copper for electrochemical-mechanical polishing applications [J]. Transactions of Nonferrous Metals Society of China, 2009, 19: 262–265.
- [3] LEE S J, LEE Y M, DU M F. The polishing mechanism of electrochemical mechanical polishing technology [J]. Journal of Materials Processing Technology, 2003, 140: 280–286.
- [4] TILEY J, SHIVELEY K, VISWANATHAN G B, CROUSE C A, SHIVELEY A. Novel automatic electrochemical-mechanical polishing (ECMP) of metals for scanning electron microscopy [J]. Micron, 2010, 41: 615–621.
- [5] TU G C, HUANG C A. The electrochemical polishing behavior of porous austenitic stainless steel (AISI 316L) in phosphoric-sulfuric mixed acids [J]. Surface & Coatings Technology, 2005, 200: 2065–2071.
- [6] CHEN S C, HONG T, OGUSHI T, NAGUMO M. The effect of chromium enrichment in the film formed by surface treatments on the corrosion resistance of type 430 stainless steel [J]. Corrosion Science, 1996, 38(6): 881–888.
- [7] LÜ W L, CHEN T J, MA Y, XU W J, YANG J, HAO Y. Effects of increase extent of voltage on wear and corrosion resistance of micro-arc oxidation coatings on AZ91D alloy [J]. Materials Chemistry and Physics, 2008, 18: 354–360.
- [8] ZHANG R F, SHAN D Y, HAN E H, GUO S B. Development of microarc oxidation process to improve corrosion resistance on AZ91 HP magnesium alloy [J]. Transactions of Nonferrous Metals Society of China, 2006, 16: 685–688.
- [9] STOYCHEV D, STEFANOV P, NICOLOVA D, VALOVA I, MAFINOVA T S. Chemical composition and corrosion resistance of passive chromate films formed on stainless steels 316L and 1.4301 [J]. Materials Chemistry and Physics, 2002, 73: 252–258.

(Edited by CHEN Wei-ping)